CORTEX 60 (2014) 34–51

Available online at www.sciencedirect.com

ScienceDirect

Journal homepage: www.elsevier.com/locate/cortex

Special issue: Research report

Selective attention modulates high-frequency activity in the face-processing network

Kathrin Müsch [a,*], Carlos M. Hamamé [b], Marcela Perrone-Bertolotti [c,d], Lorella Minotti [e], Philippe Kahane [e], Andreas K. Engel [a], Jean-Philippe Lachaux [f,g,1] and Till R. Schneider [a,1]

[a] Department of Neurophysiology and Pathophysiology, University Medical Center Hamburg-Eppendorf, Hamburg, Germany
[b] Laboratoire de Psychologie Cognitive, Aix-Marseille University, Marseille, France
[c] Université Grenoble Alpes, LPNC, Grenoble, France
[d] CNRS, LPNC, UMR, 5105 Grenoble, France
[e] Department of Neurology, Grenoble University Hospital, Grenoble, France
[f] INSERM U1028, Brain Dynamics and Cognition Team, Lyon Neuroscience Research Center, Lyon, France
[g] University Claude Bernard, Lyon, France

ARTICLE INFO

Article history:
Received 8 May 2013
Reviewed 8 December 2013
Revised 17 March 2014
Accepted 10 June 2014
Published online 20 June 2014

Keywords:
Emotion
Face processing
Amygdala
Gamma band activity
Intracranial EEG

ABSTRACT

Face processing depends on the orchestrated activity of a large-scale neuronal network. Its activity can be modulated by attention as a function of task demands. However, it remains largely unknown whether voluntary, endogenous attention and reflexive, exogenous attention to facial expressions equally affect all regions of the face-processing network, and whether such effects primarily modify the strength of the neuronal response, the latency, the duration, or the spectral characteristics. We exploited the good temporal and spatial resolution of intracranial electroencephalography (iEEG) and recorded from depth electrodes to uncover the fast dynamics of emotional face processing. We investigated frequency-specific responses and event-related potentials (ERP) in the ventral occipito-temporal cortex (VOTC), ventral temporal cortex (VTC), anterior insula, orbitofrontal cortex (OFC), and amygdala when facial expressions were task-relevant or task-irrelevant. All investigated regions of interest (ROI) were clearly modulated by task demands and exhibited stronger changes in stimulus-induced gamma band activity (50–150 Hz) when facial expressions were task-relevant. Observed latencies demonstrate that the activation is temporally coordinated across the network, rather than serially proceeding along a processing hierarchy. Early and sustained responses to task-relevant faces in VOTC and VTC corroborate their role for the core system of face processing, but they also occurred in the anterior insula. Strong attentional modulation in the OFC and amygdala (300 msec) suggests that the extended system of the face-processing network is only recruited if the

* *Corresponding author*. Department of Neurophysiology and Pathophysiology, University Medical Center Hamburg-Eppendorf, Martinistraße 52, 20246, Hamburg, Germany.
E-mail addresses: kathrin.muesch@gmail.com (K. Müsch), carlos-miguel.hamame@univ-amu.fr (C.M. Hamamé), perronemarcela@gmail.com (M. Perrone-Bertolotti), LMinotti@chu-grenoble.fr (L. Minotti), philippe.kahane@ujf-grenoble.fr (P. Kahane), ak.engel@uke.de (A.K. Engel), jp.lachaux@inserm.fr (J.-P. Lachaux), t.schneider@uke.de (T.R. Schneider).
[1] These authors contributed equally to this work.
http://dx.doi.org/10.1016/j.cortex.2014.06.006

task demands active face processing. Contrary to our expectation, we rarely observed differences between fearful and neutral faces. Our results demonstrate that activity in the face-processing network is susceptible to the deployment of selective attention. Moreover, we show that endogenous attention operates along the whole face-processing network, and that these effects are reflected in frequency-specific changes in the gamma band.

1. Introduction

Emotionally and socially significant stimuli in our environment receive prioritized perceptual processing. This processing bias has been attributed to the engagement of reflexive, exogenous attention (Vuilleumier, 2005) and entails an adaptive advantage for the organism (Öhman & Mineka, 2001). Facial expressions are among the most emotionally and socially significant stimuli in the human environment because they signify intentions and emotional states of our conspecifics, making them essential for social communication. This has led to the hypothesis that a processing bias for emotional facial expressions is hard-wired into the human brain (Palermo & Rhodes, 2007).

Processing of faces in general and emotional facial expressions in particular depend on the orchestrated activity of large-scale neuronal networks (Gobbini & Haxby, 2007; Haxby, Hoffman, & Gobbini, 2000; Vuilleumier & Pourtois, 2007). A study using functional magnetic resonance imaging (fMRI) in humans identified a network of face-responsive regions involving the inferior occipital gyrus, the fusiform gyrus, the superior temporal sulcus, the amygdala, the hippocampus, the inferior frontal gyrus, and the orbitofrontal cortex (OFC) (Ishai, Schmidt, & Boesiger, 2005), confirming the importance of these regions for face processing. The visual perception of faces has been attributed to occipital and temporal regions including the inferior occipital, the fusiform, and the inferior temporal gyri (Kanwisher, McDermott, & Chun, 1997; Parvizi et al., 2012; Pourtois, Spinelli, Seeck, & Vuilleumier, 2010a; Tsuchiya, Kawasaki, Oya, Howard, & Adolphs, 2008). However, the face-processing network can be dynamically extended with regions recruited for the extraction of specific aspects of a face depending on the task or context at hand. Consequently, the terms "core system" and "extended system" have been coined to describe networks involved in basic visual perception and subsequent, context-related analysis of faces, respectively (Gobbini & Haxby, 2007; Haxby et al., 2000). Processing of facial expressions involves the core system and additional parts of the extended system such as the amygdala, the insula, and the OFC. Previous accounts ascribed a dominant role to the amygdala in processing especially fearful faces (Adolphs, Tranel, Damasio, & Damasio, 1994; Cornwell et al., 2008; Krolak-Salmon, Hénaff, Vighetto, Bertrand, & Mauguière, 2004; Morris et al., 1996; Pourtois, Spinelli, Seeck, & Vuilleumier, 2010b; Vuilleumier, Richardson, Armony, Driver, & Dolan, 2004). More recent work showed that amygdala activity (1) is not limited to fearful facial expressions but can also be found with faces depicting neutral or happy expressions and (2) can be subsumed under processing stimulus relevance or significance (Adolphs, 2010; Canli, Sivers, Whitfield, Gotlib, & Gabrieli, 2002; Fusar-Poli et al., 2009; Rutishauser et al., 2011; Sander, Grafman, & Zalla, 2003). The OFC is involved in identification of facial expressions and their associated meaning (Adolphs, 2002; Rolls, 2004). The anterior portion of the insula has been associated with the perception of facial disgust (Fusar-Poli et al., 2009; Phillips et al., 1998) and salience detection (Menon & Uddin, 2010). Converging evidence comes from studies investigating non-human primates: face-selective clusters have been found in the temporal lobe, referred to as the anterior and middle face patch (Tsao, Freiwald, Tootell, & Livingstone, 2006; Tsao & Livingstone, 2008), in the frontal lobe (Tsao, Schweers, Moeller, & Freiwald, 2008), and in the amygdala (Gothard, Battaglia, Erickson, Spitler, & Amaral, 2007; Hoffman, Gothard, Schmid, & Logothetis, 2007; Leonard, Rolls, Wilson, & Baylis, 1985). In summary, the ventral occipito-temporal cortex (VOTC), the amygdala, the OFC, and the anterior insula form a network that mediates both perceptual processing and detailed analysis of facial expressions for further guidance of behavior.

Although some studies show that emotional facial expressions capture attention automatically (Fenker et al., 2010; Vuilleumier, 2002), the activity of the face-processing network can be modulated by voluntary, endogenous attention such as task demands or the specific context at hand. For example, Monroe et al. (2013) reported larger amplitudes of the magnetic counterpart of the N170, a prominent event-related component reflecting face processing (Bentin, Allison, Puce, Perez, & McCarthy, 1996), for fearful than for happy or neutral faces in the fusiform gyrus but only when attention had to be directed to the faces' expression and not to their age. The authors concluded that a valence modulation in the fusiform gyrus is more likely under conditions of directed attention to facial expressions. Likewise, larger event-related potentials (ERP) in the amygdala were observed specifically for fearful faces in an intracranial electroencephalography (iEEG) study, but only when the patients had to pay attention to the facial expression and not to gender (Krolak-Salmon et al., 2004). Results from a meta-analysis of fMRI data further support the notion that directed attention to facial expression boosts activity within the core and extended face-processing network. Specifically, explicit compared to implicit processing of facial expressions was associated with stronger responses in the fusiform gyrus, the amygdala, and inferior frontal regions (Fusar-Poli et al., 2009). Moreover, attentional capture by emotion is not limited to visual stimuli, such as faces, and has been reported for auditory and audiovisual

Table 1 – Medical history and pathological information of the sample.

Pat	Epileptic focus		Etiology	Seizure information				Current drugs	Medical history	Resection or electrocoagulation	Post-operative deficit
	Lat	Reg		Frequency (multiple seizures)	Age of onset	Clinical manifestations	LOC				
P1	RH	Middle temporal lobe, hippocampal sclerosis	Cryptogenic	Monthly	3	Epigastric sensation, throat discomfort, ictal dysphonia	Yes	CBZ, LTG	Major depression, anxiety disorders (panic attack)	Anterio-medial temporal lobe	NR
P2	LH	Frontal lobe	Cortical dysplasia	Weekly	8	Speech arrest, motor sensation	No	ZNS, LCS, PHT	NR	Fronto-opercular cortex	Anarthria
P3	RH	Temporo-parietal lobe	Heterotopia	Weekly	12	Aura, déjà-vu, out-of-body sensation	Yes	VPA, CBZ	NR	Electrocoagulation	NR
P4	LH	Middle temporal lobe	Cryptogenic	Daily	5	Hypomotor seizure	Yes	LTG, LCS	NR	Anterior temporal lobe, hippocampus	Transitory anomia
P5	RH	Basal frontal cortex	Cryptogenic	Monthly	10	Epigastric sensation, ictal dysphonia, vocal automatisms	Yes	LEV, LCS, OXC	NR	Prefrontal pole, medial prefrontal cortex	NR
P6	LH	Middle temporal lobe	Cryptogenic	Weekly	17	Hot sensation spreading from thorax to face	Yes	LCS, CLB, LTG	Interictal anomia	Temporal cortectomy	Transitory anomia
P7	LH	Basal temporal lobe	Cryptogenic	Weekly		Inconstant rotatory vertigo, vocal automatisms	Yes	OXC, CLE	NR	Anterior temporal lobe	NR
P8	LH	Fronto-temporal lobe	Cryptogenic	Weekly	26	Partial loss of consciousness, happy sensation	Yes	LEV, LTG, LCS	NR	Anterior temporal lobe, Frontal pole, orbital cortex	Anomia
P9	RH	Basal temporal lobe	Cryptogenic	Monthly	16	Warm feeling	Yes	OXC, LCS	NR	Electrocoagulation	NR
P10	LH	Middle temporal lobe	Cryptogenic	Monthly	17	Speech arrest and automatisms	Yes	LCS, LTG	NR	Temporo-parietal junction	Anomia

Abbreviations: CBZ, carbamazepine; CLB, clobazam; CLE, clonazepam; Lat, lateralization; LCS, lacosamide; LEV, levetiracetam; LH, left hemisphere; LOC, loss of control; LTG, lamotrigine; NR, nothing to report; OXC, oxcarbazepine; Pat, patient; PHT, phenytoin; Reg, brain region; RH, right hemisphere; VPA, sodium valproate; ZNS, zonisamide.

stimuli both of negative and positive valence especially in temporal and frontal brain regions (Grandjean, Sander, Lucas, Scherer, & Vuilleumier, 2008; Kreifelts, Ethofer, Grodd, Erb, & Wildgruber, 2007; Sander et al., 2005). In particular, results of a cross-modal dot-probe paradigm revealed that emotional prosody modulated visual target processing in occipital cortex around 100 msec (Brosch, Grandjean, Sander, & Scherer, 2009).

iEEG recordings allow the investigation of face processing with precise information on the temporal structure (e.g., latency, duration) of neuronal responses. This temporal information is obtained with high spatial precision, as electrodes are directly placed within targeted neuronal populations. Furthermore, the neuronal responses recorded with iEEG can be analyzed with respect to their spectral components, reflecting different processes. It has been suggested that dynamic interactions of cell assemblies, reflected in temporal synchronization of neuronal activity, provide indices of network interactions (Engel, Fries, & Singer, 2001; Siegel, Donner, & Engel, 2012). In the local field potential, gamma band activity (GBA; >30 Hz) has been related to local oscillatory activity (Donner & Siegel, 2011), population level spiking activity (Lachaux, Axmacher, Mormann, Halgren, & Crone, 2012; Manning, Jacobs, Fried, & Kahana, 2009; Ray & Maunsell, 2011), and the hemodynamic responses measured with fMRI (Lachaux et al., 2007; Logothetis, Pauls, Augath, Trinath, & Oeltermann, 2001). Directed attention reliably increases GBA and concomitantly decreases lower frequencies in the alpha (8–12 Hz) and beta (13–30 Hz) band (Fries, Reynolds, Rorie, & Desimone, 2001; Jensen, Kaiser, & Lachaux, 2007; Ossandón et al., 2012; Siegel, Donner, Oostenveld, Fries, & Engel, 2008). GBA has been related to the perception (Rodriguez et al., 1999) and structural encoding of faces (Gao et al., 2013; Zion-Golumbic & Bentin, 2007). Furthermore, processing emotional compared to neutral facial expressions elicited power changes in the delta (.5–4 Hz), theta (4–8 Hz), and gamma band (Balconi & Lucchiari, 2006; Balconi & Pozzoli, 2007). Studies using either iEEG or electrocorticography (ECoG) with subdural grids or strips revealed that (emotional) face processing has been associated with specific ERP components (Allison, McCarthy, Nobre, Puce, & Belger, 1994; Allison, Puce, Spencer, & McCarthy, 1999; Halgren et al., 1994; Krolak-Salmon et al., 2004; McCarthy, Puce, Belger, & Allison, 1999; Pourtois et al., 2010a, 2010b; Puce, Allison, & McCarthy, 1999). Few intracranial studies investigated modulation of frequency-specific neuronal responses in the face-processing network (Engell & McCarthy, 2010, 2011; Lachaux et al., 2005; Tsuchiya et al., 2008; Vidal et al., 2010). Only one research group examined synchronization of GBA in response to neutral (Sato et al., 2012) and fearful facial expressions (Sato et al., 2011b). However, these experiments were confined to the amygdala and did not investigate attentional modulation. Here we investigated whether directing attention towards or away from facial expressions is associated with fast changes of neuronal activity in the face-processing network.

To address this question, we recorded from depth electrodes implanted in patients undergoing resective neurosurgical treatment for drug-resistant epilepsy in order to uncover the fast dynamics of emotional face processing. We investigated frequency-specific neuronal activity and ERPs in different regions of the face-processing network: the VOTC (including the posterior fusiform gyrus) and ventral temporal cortex (VTC; including the anterior inferior temporal gyrus), the anterior insula, the OFC, and the amygdala. We compared neuronal responses between faces and control stimuli (nonfaces) and between two facial expressions (fearful *vs* neutral) under two different detection tasks. Spatial attention was always directed toward centrally presented face and nonface stimuli. However, the attentional focus on facial expressions was manipulated by the task. The tasks demanded either to focus on the facial expressions (explicit task) or on low level features of the image (implicit task). We predicted that neuronal activity in the face-processing network can be modulated by two factors: (1) by reflexive, exogenous attention driven by stimulus salience (face > nonface, fearful > neutral) and (2) by voluntary, endogenous attention driven by task demands (explicit > implicit). We expected that task demands and facial expressions modulate the increase and duration of GBA and concomitant decreases of alpha-beta-band activity (ABBA). Furthermore, we investigated whether task demands and stimulus salience globally affect the face-processing network, or whether regions of the core and the extended system are recruited specifically.

2. Methods

2.1. Participants

We obtained intracranial recordings from ten right-handed patients with drug-resistant epilepsy (5 males, mean age, *M* ± standard deviation, *SD* = 29.6 ± 6.4 years) who were evaluated for possible surgery at the Epilepsy Department of the Grenoble University Hospital (Grenoble, France). Table 1 summarizes medical history, pathological information, current medication at the time of experiment and resected tissue for each patient. Recording sites were solely determined according to clinical considerations with no reference to the current experiment. All patients provided written informed consent. The Ethical Committee of Grenoble Sud-Est V approved the experimental procedures (Study 0907 – ISD et SEEG, CPP 09-CHUG-12). The experiments were carried out according to the Declaration of Helsinki. All patients had normal or corrected to normal vision.

2.2. Stimuli and experimental design

Twenty-seven male and 27 female faces with neutral, fearful, and happy expressions were taken from the Karolinska Directed Emotional Faces (Lundqvist, Flykt, & Öhman, 1998). All stimuli were converted to gray-scale, matched for luminance, and masked by an oval shape to remove hair, neck and background information. Phase-scrambled versions of neutral and fearful faces served as perceptual control stimuli and will be referred to as nonfaces in the following. To manipulate the allocation of attention, we ran two blocked versions of the task (Fig. 1) differing solely in whether facial expression was task-relevant or not, hence referred to as explicit and implicit task. Targets of the implicit task were fearful faces, neutral faces, or nonfaces with a red tint in order to distinguish them

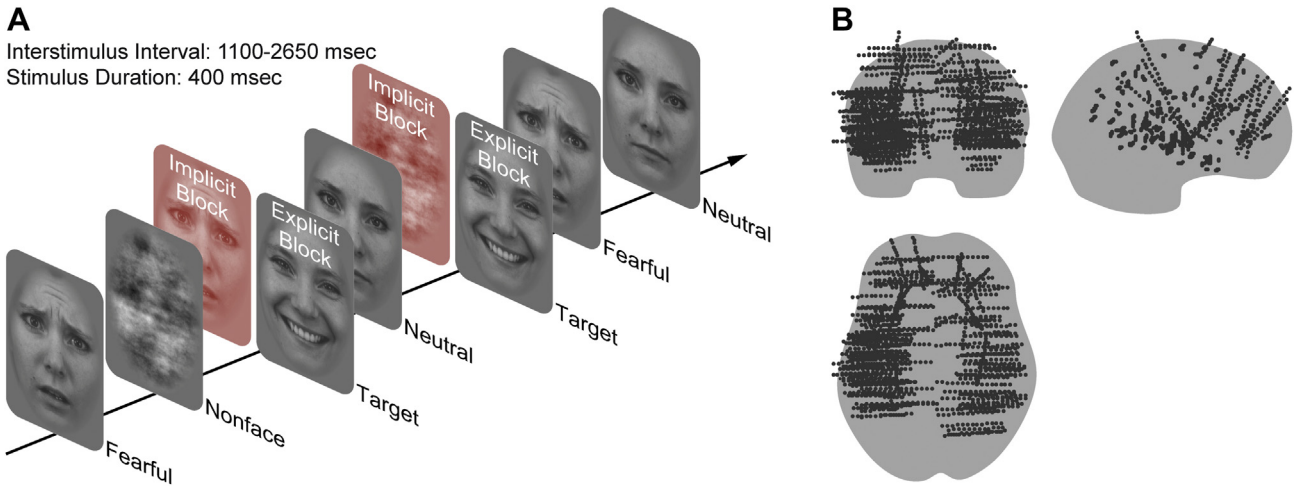

Fig. 1 – (A) Schematic of implicit and explicit tasks. Tasks differed solely in the type of target and the task instructions. Patients had to detect stimuli with a red tint and happy faces in implicit and explicit tasks, respectively. (B) Electrode coverage of the entire brain across all patients in a MNI glass brain.

from the other stimuli in the stream, while targets of the explicit task were gray-scale faces with happy expressions. In both tasks, all visual stimuli were presented randomly for 400 msec with a jittered interstimulus interval (1100–2650 msec). In the implicit task, patients had to detect the stimuli with the red tint, whereas in the explicit task faces with happy expressions had to be detected and reported by a button press. It was intended that targets in the explicit task should be as well detected as targets in the implicit task. Therefore, happy facial expressions were chosen as targets because they yield higher recognition scores than any other facial expression (Russell, 1994). Happy faces were not included in the implicit task, since we were particularly interested in differential processing of fearful and neutral faces and wanted to maximize the number of trials per condition of interest. Only 10% of the trials consisted of targets to maintain attention throughout the task. Target stimuli were discarded from further analysis. In each block, 180 trials consisting of 54 nonfaces, half fearful-scrambled and half neutral-scrambled, 54 neutral, 54 fearful faces and 18 targets were presented. In each implicit task block targets consisted of 18 stimuli with red tint (6 neutral faces, 6 fearful faces, and 6 nonfaces). Implicit task blocks always preceded explicit task blocks to minimize bias for facial expression. The whole set of implicit and explicit task blocks was repeated when possible. In total, every patient performed each task twice, except for patient 2 (P2). Visual stimuli subtended $10^\circ \times 16^\circ$ visual angle and were displayed on a 22″ TFT monitor at a refresh rate of 60 Hz and a viewing distance of approximately 60 cm using Presentation (Neurobehavioral Systems, Albany, CA, USA).

2.3. *Electrode implantation and localization*

Thirteen to 16 semirigid, multilead electrodes were stereotactically implanted in each patient. All electrodes had a diameter of .8 mm with 5–18 contacts, each of 2 mm length and 1.5 mm apart (Dixi, Besançon, France).

The experiment was conducted five to seven days ($M \pm SD = 6.0 \pm .5$) following electrode implantation. The location of each site was determined by coregistration of the individual pre- to postimplantation structural MRI and normalization of the preimplantation MRI to the International Consortium for Brain Mapping template (Montreal Neurological Institute [MNI], Montreal, Canada). Electrode localization was performed with SPM8 (http://www.fil.ion.ucl.ac.uk/spm/) and nutmeg (http://nutmeg.berkeley.edu). Anatomical regions were identified with the automated anatomical labeling atlas (Tzourio-Mazoyer et al., 2002) with MRIcron (http://www.mccauslandcenter.sc.edu/mricro/mricron/). All coordinates (x, y, z in mm) are given in MNI space (Evans et al., 1993).

2.4. *Stereotactic EEG recordings and preprocessing*

The iEEG was recorded using a 128-channel video-EEG acquisition and monitoring system (Micromed, Treviso, Italy). Data were bandpass filtered online between .1 and 200 Hz and sampled at 512 Hz. A monopolar reference in the white matter was used for all contact sites during data acquisition and for analyses of the ERPs. For the spectral analyses, each contact was re-referenced offline to its adjacent neighbor on the same electrode. In the following, these data will be referred to as "sites"; electrodes are labeled by lower case letters and sites by numbers; apostrophes mark electrodes in the left hemisphere. This bipolar reference montage increases local specificity by suppressing signal artifacts from adjacent recording sites and effects due to volume conduction (Jerbi, Freyermuth, et al., 2009; Jerbi, Ossandón, et al., 2009; Lachaux, Rudrauf, & Kahane, 2003). Spatial resolution after bipolar referencing is below intercontact spacing (i.e., 3.5 mm). Data were systematically screened for epileptiform activity using visual and semiautomatic inspection. Any trial containing epileptiform activity was discarded from further analysis. Bipolar referenced data were high-pass filtered at .5 Hz and low-pass filtered at

170 Hz for spectral analysis. For computation of ERPs, monopolar referenced data were high-pass filtered offline at .5 Hz and low-pass filtered at 25 Hz. The recorded signal was epoched into segments of −500 to 1000 msec around stimulus onset. Data analysis was performed with custom MATLAB (The Mathworks, Natick, MA, USA) routines and FieldTrip (Oostenveld, Fries, Maris, & Schoffelen, 2011).

2.5. Data analysis

2.5.1. Behavioral data

The percentage of hits was calculated as the proportion of detected targets relative to the total number of targets. The percentage of false alarms was defined as the proportion of nontargets followed by button presses. Low values of false alarms indicate that participants were able to perform the task correctly. Hits and false alarms were computed separately for implicit and explicit tasks. In order to assess the sensitivity, d′ was calculated according to signal detection theory as d′ = Z(hit rate)−Z(false alarm rate), with Z being the inverse of the cumulative Gaussian distribution (Macmillan & Creelman, 1991). In cases of perfect performance, d′ was estimated assuming that 1/100th of the performance was wrong (Wickens, 2002). Mean reaction times were computed for explicit and implicit tasks. Paired *t* tests compared the d' scores and reaction times of both tasks.

2.5.2. Selection of sites

Visually responsive sites were determined based on the GBA responses (50–150 Hz) because the high frequency range has been previously associated with visual processing of complex stimuli (Lachaux et al., 2012, 2005; Ossandón et al., 2012; Tsuchiya et al., 2008; Vidal et al., 2010). First, the instantaneous amplitude at 50–150 Hz was estimated using the Hilbert transform (for further details, please see 2.5.3). Second, the GBA of trials from all conditions (fear, neutral, nonface) and tasks (explicit, implicit) was collapsed. Third, each poststimulus sample point of this average response was compared to the mean of the prestimulus baseline (−400 to −100 msec) with a Wilcoxon signed rank test running across poststimulus sample points. To account for multiple testing, the obtained *p* values were corrected with the false discovery rate (FDR) at $p < .05$ (Benjamini & Hochberg, 1995). In addition, at least three subsequent sample points had to be significant after FDR correction to reflect a meaningful visual response. Finally, visually responsive sites were selected in a-priori defined regions of interest (ROI). Regions were selected based on meta-analytic, functional neuroimaging data on processing of facial expressions or emotion (Fusar-Poli et al., 2009; Phan, Wager, Taylor, & Liberzon, 2002) and included the VOTC, the VTC anterior to the VOTC, the anterior insula, the OFC, and the amygdala. The labels of the automated anatomical labeling atlas (Tzourio-Mazoyer et al., 2002) guided anatomical delineation of sites included in a given ROI, and the exact position of the sites was confirmed in the individual MRIs if necessary. Only sites matching the selection criterion described above were considered for subsequent analysis including ABBA power profiles and ERPs. Since contacts in the amygdala were rare, those sites were considered irrespectively of exceeding the selection threshold.

2.5.3. Spectral analyses

Spectral analyses included two separate methods: (1) computation of time-frequency representations (TFR) using a sliding-time-window Fourier transformation, and (2) an estimation of the instantaneous amplitude using the Hilbert transform of bandpass filtered signals (Le Van Quyen et al., 2001). For TFR plots, Hanning windows were applied for low frequencies (2.5–30 Hz), and the multitaper method based on discrete prolate spheroidal (Slepian) tapers (Mitra & Pesaran, 1999) was used for high frequencies (30–150 Hz). The Fourier transformation was calculated for each of the tapers, and the spectra for each individual taper were magnitude squared. The power for each tapered data segment was then averaged. Each trial was zero padded up to 2 sec of length. The length of the sliding time window ΔT and the amount of spectral smoothing Δf determines the number of tapers $k = [(\Delta T * \Delta f) - 1]$. For the analysis of low (2.5–30 Hz in steps of 2.5 Hz) and high frequencies (30–150 Hz in steps of 10 Hz), sliding time windows of fixed length ($\Delta T = 400$ msec and $\Delta T = 200$ msec, respectively) with a step size of 20 msec and fixed frequency smoothing ($\Delta f = 2.5$ Hz and $\Delta f = 20$ Hz, respectively) were used, computed with a single taper for low and three tapers for high frequency ranges. For total power, frequency decomposition was performed on single-trial data, and power values of single trials were then averaged. These power estimates can include signal components that are phase-locked and non phase-locked to the stimulus onset (Tallon-Baudry & Bertrand, 1999). Furthermore, responses were characterized as the percentage of signal change according to the formula: total power = $\text{poststimulus}_{\text{total}}$−$\text{prestimulus}_{\text{total}}$. In order to avoid an overlap of the baseline window with the poststimulus window, the baseline period spanned from −500 msec to [stimulus onset−½ΔT], with $\Delta T = 400$ msec for low and $\Delta T = 200$ msec for high frequencies, respectively. Thus, the baseline period differed for high and low frequencies. TFR plots were estimated for all sites that were included in a given ROI. For each ROI, activity was first averaged across all sites in a single patient before it was collapsed across patients. For visualization, the poststimulus period of each condition and frequency range was separately tested against the mean prestimulus period with a dependent samples *t*-test, and the resulting *t* values were transformed into *z*-scores. In addition, the difference between faces and nonfaces of each task and frequency range was separately assessed by means of a dependent samples *t*-test, and the resulting *t* values were transformed into *z*-scores. The TFRs were used for visualization and to verify that the main responses were in the frequency bands of interest (cf. below).

Based on previous research on visual and attentional responses (Lachaux et al., 2005; Ossandón et al., 2012; Tsuchiya et al., 2008; Vidal et al., 2010), we restricted the Hilbert transformation approach to frequencies between 8 and 24 Hz (ABBA) and to frequencies between 50 and 150 Hz (GBA). Tsuchiya et al. (2008) utilized a decoding approach to identify the frequency bands best describing the differences between faces and control stimuli instead of a-priory specifying a frequency band of interest. This decoding approach revealed that exactly the frequency range between 50 and 150 Hz optimally described the differences between faces and control stimuli. Applying the Hilbert transform to continuous recordings splits

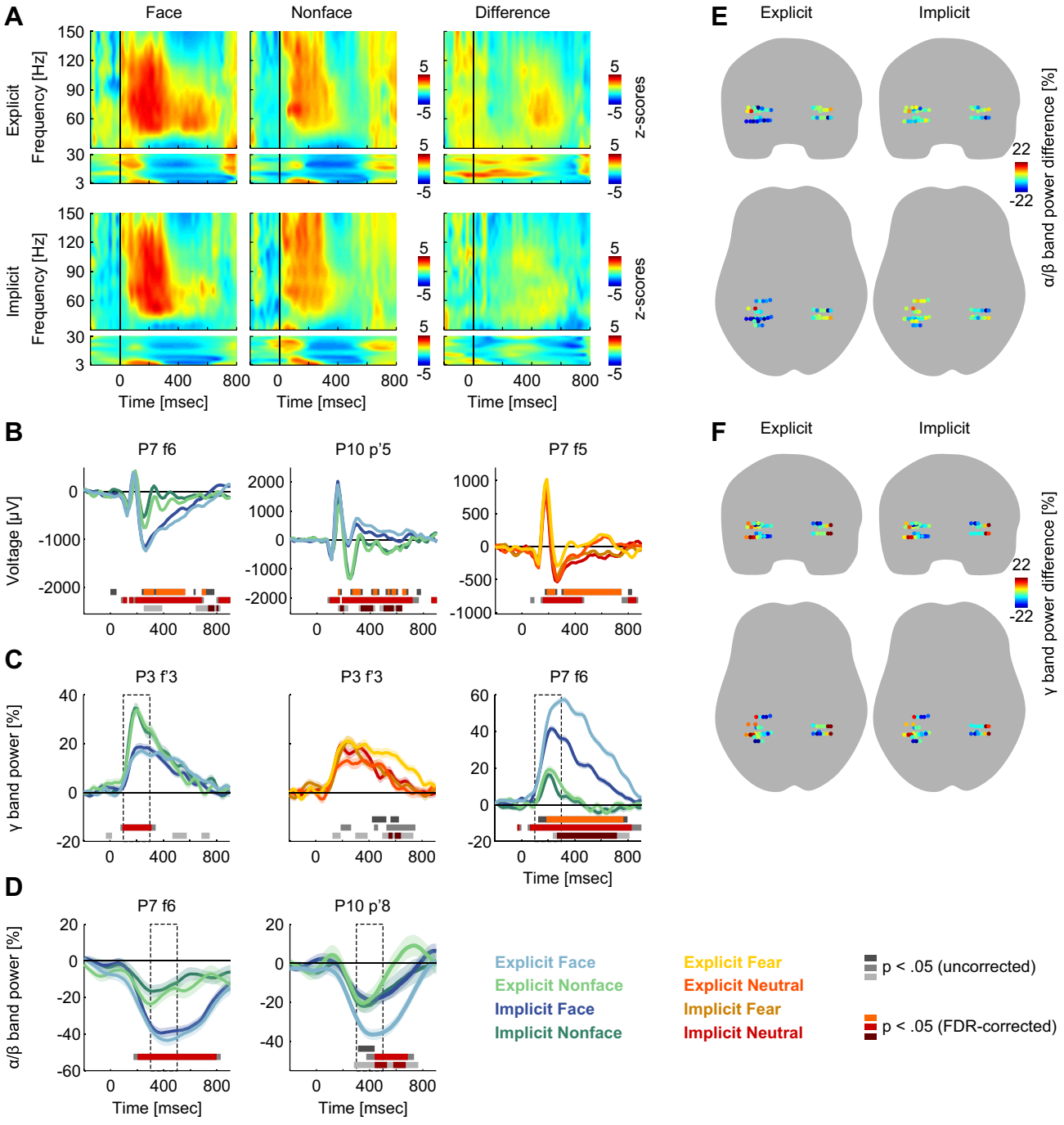

Fig. 2 – Results for the VOTC. (A) TFR averaged across all sites included in the VOTC for the conditions face, nonface, and their difference for explicit (upper panel) and implicit tasks (lower panel). (B) The ERPs are shown for three sites of two patients. The bars illustrate the uncorrected and FDR-corrected results of the ANOVA, color-coded for the main effect of task (top), condition (middle), and their interaction (bottom). Face *vs* nonface condition effects are indicated in the two leftmost plots and fearful *vs* neutral condition effects in the rightmost one. (C) Power profiles for GBA are depicted for two sites of two patients. The shading reflects the standard error of the mean (SEM). Face *vs* nonface condition effects are indicated in the two outer plots and fearful *vs* neutral condition effects in the middle one (statistics as described above). (D) Power profiles for ABBA are shown for two patients. The shading reflects the SEM. Face *vs* nonface condition effects are indicated (statistics as described above). (E) Mean ABBA power difference (faces minus nonfaces) separately for explicit and implicit tasks between 300and 500 msec after stimulus onset (cf. dashed rectangles in D). Depicted are all visually responsive sites in the VOTC across patients. (F) Mean GBA power difference (faces minus nonfaces) separately for explicit and implicit tasks between 100and 300 msec after stimulus onset (cf. dashed rectangles in C) for the same sites.

the data into instantaneous amplitude (i.e., envelope) and phase components in the frequency ranges of interest (Le Van Quyen et al., 2001). The continuous iEEG signal was bandpass filtered in multiple successive frequency bands (from 50 to 150 Hz in steps of 10 Hz or from 8 to 24 Hz in steps of 4 Hz for high and low frequencies, respectively) using a zero phase shift, noncausal, finite impulse filter with .5 Hz roll-off. Then, the envelopes, i.e., the time-varying amplitude, for each bandpass filtered signal were computed with the standard Hilbert transform. The envelope of each frequency band was divided by its mean across the entire recording session and multiplied by 100, yielding responses expressed in percentage of the mean (%). This normalization procedure accounted for a bias towards lower frequencies due to the power law. Finally, the envelopes of all multiple successive frequency bands were averaged providing one single time series across the entire session. For data reduction, the final Hilbert envelopes were down-sampled to 64 Hz. Similar to the TFRs, these power profiles were characterized as the percentage of signal change relative to baseline according to GBA = [(poststimulus$_{GBA}$−prestimulus$_{GBA}$)/prestimulus$_{GBA}$] and ABBA = [(poststimulus$_{ABBA}$−prestimulus$_{ABBA}$)/prestimulus$_{ABBA}$]. The baseline period spanned from −400 msec to −100 msec before stimulus onset. As an additional level of confidence, the power profile computation using the Hilbert transform was also used to confirm the TFRs obtained by the sliding window approach. However, all statistical analyses were performed on the power profiles obtained by the Hilbert transformation because they provide a lower degree of complexity and thus higher statistical power. For visualization on the population level, the average power profile for a specific time window of interest (e.g., 100–300 msec) was computed separately for faces and nonfaces for all bipolar, visually responsive sites in a given ROI across all patients. Then the difference between faces and nonfaces was plotted at the corresponding location in the MNI brain.

2.5.4. ERPs

The segmented, monopolar-referenced signal was averaged for each condition and baseline corrected between −500 and 0 msec before stimulus onset. The ERP signal was resampled to 64 Hz to assure comparable resolution to the Hilbert envelopes for statistical analysis.

2.5.5. Statistics

Statistical analysis of electrophysiological data was performed at the single site level (Lachaux et al., 2012, 2005) for all selected contacts. A two-way analysis of variance (ANOVA) with the factors task and condition was performed separately for each neuronal marker (GBA, ABBA, ERP) time-resolved for each poststimulus sample point. Since differences between faces, i.e., the average of fearful and neutral faces, and nonfaces dominated and occluded differences between fearful and neutral faces, when all three conditions were included as levels of the experimental factor condition, two separate ANOVAs (nonrepeated measures) were calculated to disentangle the influence of the face per se from that of the emotional expression. The first ANOVA compared task (explicit, implicit) with condition (face, nonface), whereas the second ANOVA contrasted task (explicit, implicit) with condition (fear, neutral). Specifically, separate two-way ANOVAs including the two experimental factors (task by condition) were computed for each poststimulus sample point (each 15.625 msec) of the baseline-corrected, single-trial data. The resulting p values for the main effects of task and condition and of their interaction were separately FDR-corrected across all poststimulus sample points to account for multiple comparisons.

3. Results

3.1. Behavioral performance

The mean hit and false alarm rates ($M \pm SD$) were 87.8% ± 13.8; and 1.2% ± 1.3 for the explicit task and 96.1% ± 7.6 and .7% ± 1.7 for the implicit task. The sensitivity index d' did not differ between tasks (explicit: $M \pm SD = 3.7 \pm .9$; implicit: $M \pm SD = 4.3 \pm .6$; $t_9 = -2.02$, $p = .074$). Patients responded faster to red-tinted targets in the implicit task ($M \pm SD = 470.9$ msec ± 39.7) than to happy face targets in the explicit task ($M \pm SD = 603.5$ msec ± 70.9; $t_9 = 6.68$, $p < .001$). These results confirm that patients were able to perform the task, and suggest that the implicit task was easier than the explicit one, as reflected in the reaction times but not in the performance scores.

3.2. VOTC

In order to select sites from the VOTC, only visually responsive sites labeled as fusiform gyrus with the y coordinate ≤ −35 and the x coordinate < |45| were considered. All sites were within Brodmann areas (BA) 19 and 37. In total, 45 sites in VOTC from eight patients (P1, P3, P4, P6, P7, P8, P9, P10) were included.

In most recording sites within the VOTC (41/45), the presentation of visual stimuli resulted in a prompt, strong, and sustained GBA increase after 80 msec (Fig. 2A). Initial GBA peaks between 100 and 200 msec were stronger for faces than nonfaces (10/41), especially at lateral VOTC sites, and stronger for nonfaces than faces (19/41; Fig. 2F), especially at medial VOTC sites. This stimulus specificity resulted in a condition effect emerging after 100 msec or even earlier (cf. P3 f'3 and P7 f6, Fig. 2C). After the initial peak, the GBA response to faces compared to nonfaces in the explicit task was more sustained, while GBA in the implicit task was less sustained, resulting in a significant interaction after 250 msec and lasting up to 700 msec (11/41 sites, cf. P7 f6, Fig. 2C). Enhanced GBA to fearful compared to neutral faces was observed in two sites (300–500 msec), which was very robust at the single-trial level (cf. P3 f'3, Fig. 2C).

In most sites (40/41), the enhancement of GBA co-occurred with an ABBA suppression, starting at 100 msec and peaking around 400 msec (Fig. 2A). ABBA suppression (500–700 msec) was stronger for faces than nonfaces in the majority of sites (19/40; cf. P7 f6, Fig. 2D and E). In seven out of 40 sites, stronger ABBA suppression for faces compared to nonfaces was only present in the explicit task (cf. P10 p'8, Fig. 2D). Task effects occurred beyond 700 msec. Differential processing for fearful and neutral faces could not be observed for ABBA.

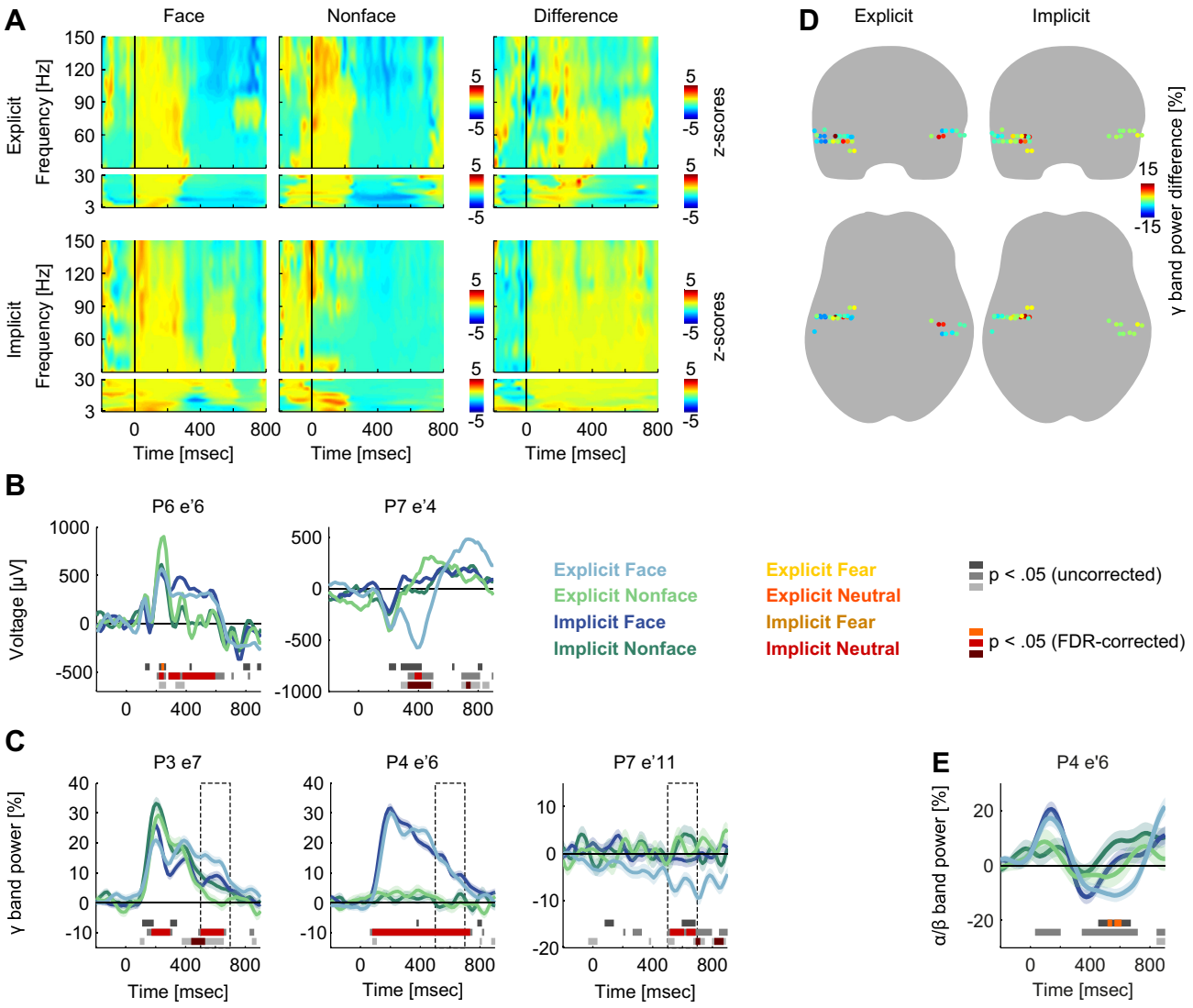

Fig. 3 – Results for the VTC. (A) TFR averaged across all sites included in the VTC for the conditions face, nonface, and their difference for explicit (upper panel) and implicit tasks (lower panel). (B) The ERPs are shown for two patients. The bars illustrate the uncorrected and FDR-corrected results of the ANOVA, color-coded for the main effect of task (top), condition (middle), and their interaction (bottom). Face *vs* nonface condition effects are depicted. (C) Power profiles for the GBA are shown for three patients (legend and statistics as described above). The shading reflects the SEM. Face *vs* nonface condition effects are depicted. (D) Mean GBA power difference (faces minus nonfaces) separately for explicit and implicit tasks between 500 and 700 msec after stimulus onset (cf. dashed rectangles in C). Depicted are all visually responsive sites in the VTC across patients. (E) Power profiles for ABBA are shown for one patient (legend and statistics as described above). The shading reflects the SEM. Face *vs* nonface condition effects are depicted.

Across all recording sites, presentation of visual stimuli was associated with a very sharp onset response 100 msec poststimulus in the ERP. Fig. 2B shows a typical P1/N1-like complex following the first negative deflection similar to the N170 recorded at the scalp. ERPs differentiated faces and nonfaces, although the direction of this effect differed (compare P7 f6 with of P10 p′5). Furthermore, task effects (explicit *vs* implicit) were observed at later latencies (>200 msec) than the stimulus-specific effects (face *vs* nonface). Interaction effects did not exhibit a consistent pattern. Only three sites exhibited a differential response for the two facial expressions (cf. P7 f5, Fig. 2B).

3.3. *VTC*

Recording sites in the VTC were selected to probe face processing at a higher level along the ventral visual stream. Only visually responsive sites were considered whose y coordinate was >−35 and that were within BA 20. In total, 33 sites from seven patients (P1, P3, P4, P6, P7, P8, P10) were included.

Four out of 33 sites in the VTC (Fig. 3A) exhibited enhanced GBA in response to faces compared to nonfaces in the same time range (100–200 msec) as in the VOTC (P4 e′6, Fig. 3C), one out of 33 sites showed the opposite pattern of stronger GBA to nonfaces compared to faces (P3 e7, Fig. 3C). The remaining

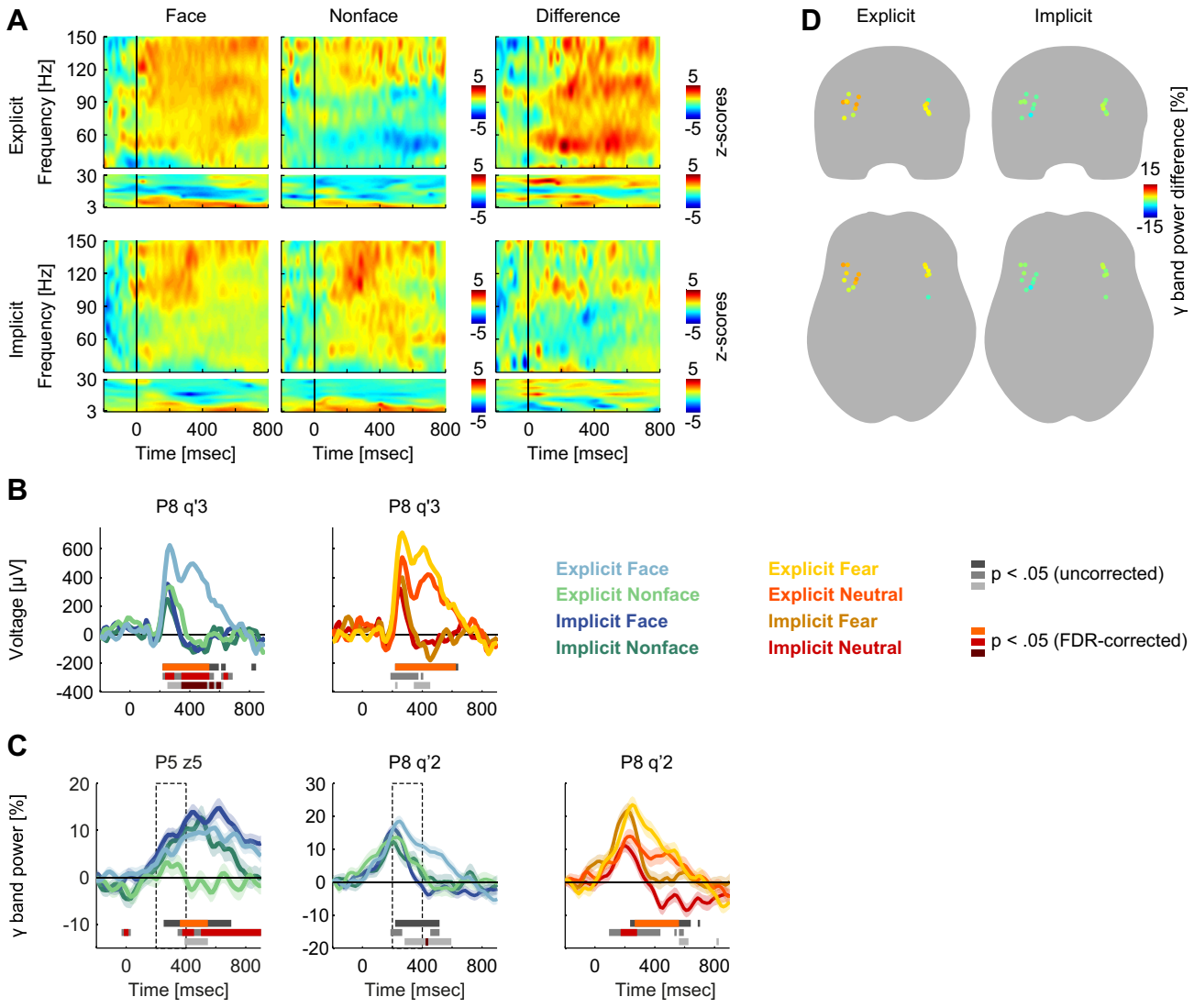

Fig. 4 – Results for the anterior insula. (A) TFR averaged across all sites included in the anterior insula for the conditions face, nonface, and their difference for explicit (upper panel) and implicit tasks (lower panel). (B) The ERPs are shown for one patient. The bars illustrate the uncorrected and FDR-corrected results of the ANOVA, color-coded for the main effect of task (top), condition (middle), and their interaction (bottom). Face *vs* nonface condition effects are indicated in the left plot and fearful *vs* neutral condition effects in the right one. (C) Power profiles for GBA are shown for two sites of two patients (legend and statistics as described above). The shading reflects the SEM. Face *vs*. nonface condition effects are indicated in the two leftmost plots and fearful *vs* neutral condition effects in the rightmost one. (F) Mean GBA power difference (faces minus nonfaces) separately for explicit and implicit tasks between 200 and 400 msec after stimulus onset (cf. dashed rectangles in C). Depicted are all visually responsive sites in the anterior insula across patients.

responses in this ROI were lower in amplitude and later in latency than in the VOTC. Additionally, GBA was more sustained in response to faces compared to nonfaces after 500 msec poststimulus during the explicit task (5/33, Fig. 3D), although the direction of this effect varied (compare P3 e7 with P7 e'11, Fig. 3C). GBA did not differ between fearful and neutral faces.

Similar to results in the VOTC, a decrease in ABBA following visual stimulation was occasionally observed in the VTC (10/33). Almost no differences between experimental conditions on ABBA suppression were found in VTC (for an exception, see Fig. 3E). Furthermore, ABBA did not differentiate between fearful and neutral faces.

ERPs in this ROI were more heterogeneous than in the VOTC. Paralleling the results in the GBA, faces compared to nonfaces elicited a more positive sustained potential 300–600 msec after stimulus onset in most of the patients (Fig. 3B). We did not observe substantial differences between explicit and implicit tasks and between fearful and neutral faces.

3.4. *Anterior insula*

Sites in the posterior insula ($y < 0$) were excluded. In total, this ROI comprised 15 visually responsive sites in four patients (P4, P5, P7, P8).

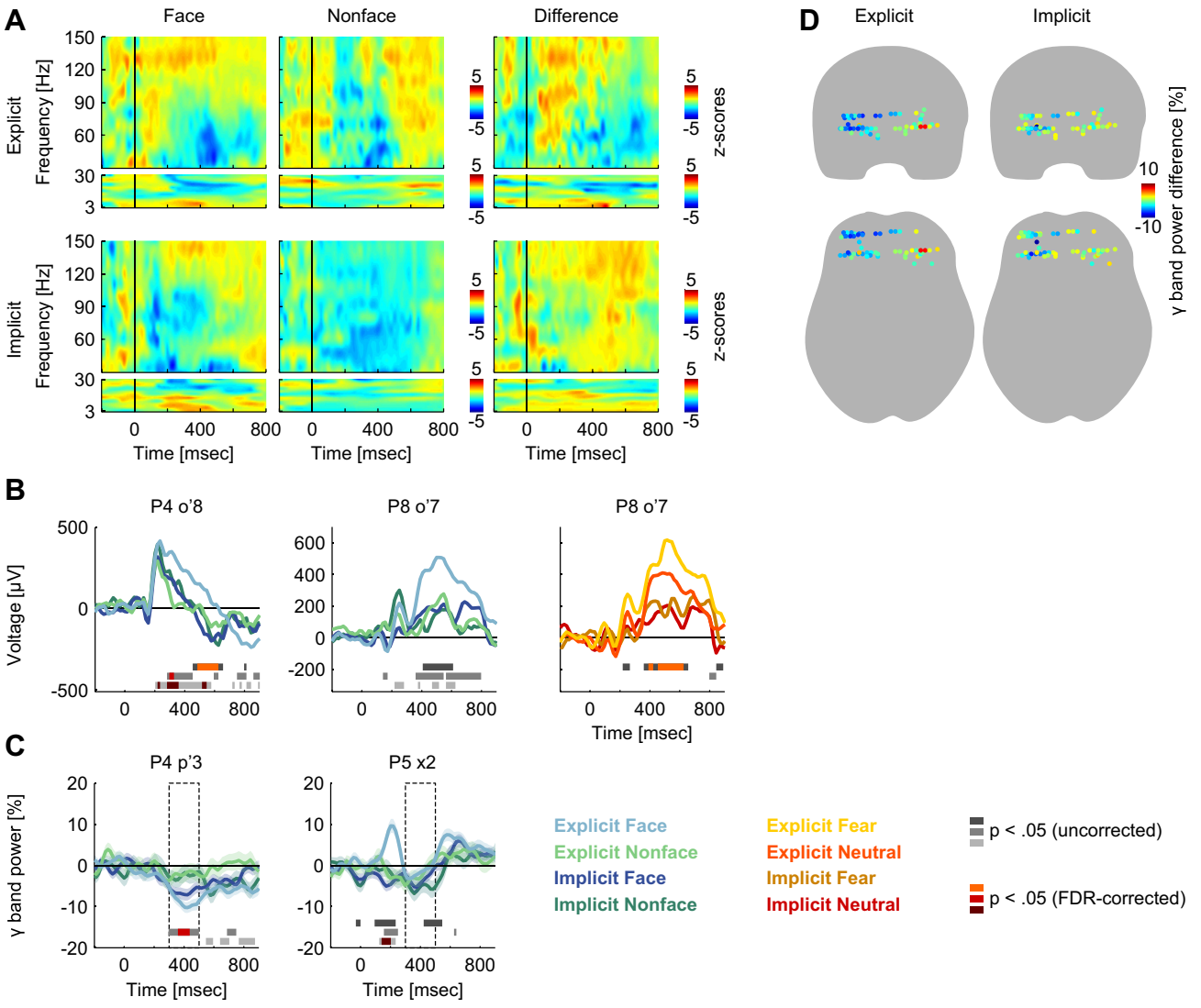

Fig. 5 – Results for the OFC. (A) TFR averaged across all sites included in the OFC for the conditions face, nonface, and their difference for explicit (upper panel) and implicit tasks (lower panel). (B) The ERPs are shown for two sites of two patients. The shading reflects the SEM. The bars illustrate the uncorrected and FDR-corrected results of the ANOVA, color-coded for the main effect of task (top), condition (middle), and their interaction (bottom). Face *vs* nonface condition effects are indicated in the two leftmost plots and fearful *vs* neutral condition effects in the rightmost one. (C) Power profiles for GBA are shown for two patients (legend and statistics as described above). (F) Mean GBA power difference (faces minus nonfaces) separately for explicit and implicit tasks between 300 and 500 msec after stimulus onset (cf. dashed rectangles in C). Shown are all visually responsive sites in the OFC across patients.

The presentation of visual stimuli yielded a strong and broadband increase in GBA at the majority of sites (10/15) that started around 100 msec (2/15) or 250 msec (8/15) and receded much slower for faces during explicit tasks than for any other condition (5/15; Fig. 4A, C, D). Differences between fearful and neutral faces paralleled the preferential processing of faces during explicit tasks, except for one site. At this site GBA initially increased to fearful faces in both task around 200 msec, followed by sustained GBA to both facial expressions in the explicit task (P8 q'2, Fig. 4C). No condition effects for ABBA were observed in this ROI.

Two patients exhibited a positive component around 200 msec in the ERP that was more pronounced for faces than for nonfaces only during the explicit task (P8 q'3, Fig. 4B). In addition, there were differences between tasks after 400 msec. The comparison of fearful and neutral facial expressions yielded differential responses for explicit and implicit tasks, although none survived the FDR correction (P8 q'3, Fig. 4B).

3.5. OFC

We recorded from 57 sites in six patients (P1, P4, P5, P6, P8, P10) within the OFC (BAs 10, 11, 47). Most sites (29/57) showed stronger suppression of GBA for faces compared to nonfaces between 200 and 800 msec (Fig. 5A; cf. P4 p'3, Fig. 5C), which survived multiple comparison correction in only six sites. At the group level, differential responses for faces compared to nonfaces were more pronounced during the explicit task

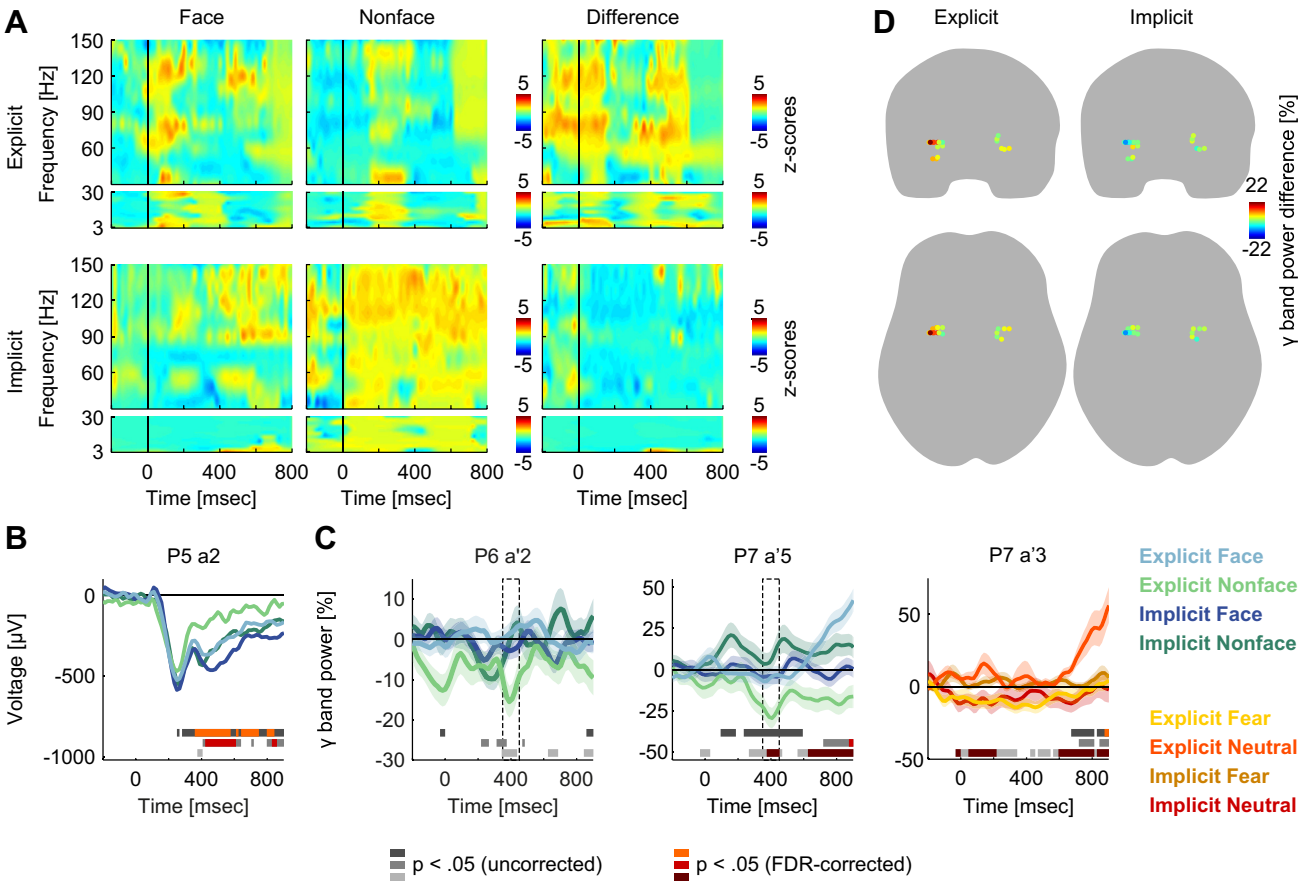

Fig. 6 – Results for the amygdala. (A) TFR averaged across all sites included in the amygdala for the conditions face, nonface, and their difference for explicit (upper panel) and implicit tasks (lower panel). (B) The ERP is shown for one patient. The bars illustrate the uncorrected and FDR-corrected results of the ANOVA, color-coded for the main effect of task (top), condition (middle), and their interaction (bottom). Face *vs* nonface condition effects are indicated. (C) Power profiles for GBA are shown for three sites of two patients (legend and statistics as described above). The shading reflects the SEM. Face *vs* nonface condition effects are indicated in the two leftmost plots and fearful *vs* neutral condition effects in the rightmost one. (D) Mean GBA power difference (faces minus nonfaces) separately for explicit and implicit tasks between 350 and 450 msec after stimulus onset (cf. dashed rectangles in C). Depicted are all sites in the amygdala across patients.

particularly in lateral sites (Fig. 5D). Interestingly, we found an early GBA enhancement exclusively for faces during the explicit task in one site of a single patient that was located medial (16, 33, −22) resulting in a significant interaction between 130 and 200 msec (P5 x2, Fig. 5C). The comparison of fearful and neutral faces did not yield any systematic effects in GBA. No effects were observed for ABBA in the OFC.

ERPs in the OFC revealed task and condition effects with varying latencies (Fig. 5B). A positive component was more sustained during face processing in the explicit task in a single patient between 300 and 550 msec (P4 o′8). The ANOVA on fearful and neutral facial expressions revealed differences between explicit and implicit tasks between 200 and 800 msec (P8 o′7, Fig. 5B).

3.6. *Amygdala*

Careful inspection of individual MRIs identified 18 sites in the amygdala of seven patients (P1, P3, P4, P5, P6, P7, P10). All sites were considered irrespective of whether they were visually responsive (cf. 2.5.2).

Four recording sites in the amygdala displayed a larger absolute difference of GBA in response to faces compared to nonfaces in explicit but not implicit tasks (Fig. 6A and D). The interaction between condition and task (350–450 msec and 600–900 msec) only survived the FDR correction in one site (P7 a′5, Fig. 6C). Only one patient exhibited stronger GBA (50–220 msec, 600–900 msec) for neutral compared to fearful faces in the explicit task, whereas no difference was found in the implicit task (P7 a′3, Fig. 6C). There were no systematic effects in the ABBA in the amygdala.

The ERPs in seven sites of the amygdala consisted of a biphasic deflection 170 msec after stimulus onset followed by a sustained negativity, which independently differed between tasks and conditions beyond 200 msec (Fig. 6B).

4. Discussion

This study investigated whether directing attention towards or away from facial expressions in a detection task was associated with fast changes of neuronal activity in the face-

processing network. Specifically, neuronal responses in the VOTC, VTC, anterior insula, OFC, and amygdala were compared when facial expressions were either task-relevant or task-irrelevant. We observed strong attentional modulation of neuronal activity during explicit face processing in all regions of the face-processing network. Endogenous, selective attention towards facial expressions modulated GBA in the VOTC, VTC, anterior insula, OFC, and amygdala. Recording sites within the VOTC and VTC exhibited early stimulus-specific responses to faces and nonfaces that were only modulated by task demands beyond 200 msec. Responses in the anterior insula showed initially stimulus-unspecific responses to faces and nonfaces, that differentiated by task demands beyond 200 msec, comparably to responses in OFC and amygdala. Except for the VOTC and VTC, in which also ABBA was suppressed, these effects were confined to the gamma band in the OFC, the anterior insula and the amygdala. The latencies of the ERPs paralleled those of GBA, while the morphology of the ERP components was more heterogeneous across subjects. Contrary to our hypothesis that fearful expression would bias exogenous attention and enhance face processing throughout the network, only a few recording sites showed reliable differences between fearful and neutral expressions beyond 200 msec. Possible reasons are discussed in more detail in 4.6.

Our results clearly demonstrate that the core system of the face-processing network (VOTC, VTC) shows early (<200 msec) stimulus-specific responses to faces and is subsequently (>200 msec) upregulated by endogenous, task-related attention. The extended system of the face-processing network (OFC, anterior insula, amygdala) is modulated by task demands. Effects of fearful facial expressions emerged beyond 200 msec in the VOTC, anterior insula, and amygdala but were small in size. GBA appears to be the most reliable neuronal marker for all of these effects.

4.1. *VOTC*

In line with previous reports in human (Engell & McCarthy, 2011; Kawasaki et al., 2012; Lachaux et al., 2005; Tsuchiya et al., 2008; Vidal et al., 2010) and nonhuman primates (Tsao et al., 2006; Tsao, Moeller, & Freiwald, 2008), responses in the VOTC were characterized by a rapid (<100 msec) increase of GBA (41 out of 45 sites), which was selective for faces in the lateral VOTC (10 out of 41 sites). Gamma band responses were accompanied by a suppression of ABBA in the majority of recording sites (Lachaux et al., 2005). Similar spectral signatures have been associated with sensory processing in the visual cortex (Engel et al., 2001; Hipp, Engel, & Siegel, 2011; Hoogenboom, Schoffelen, Oostenveld, Parkes, & Fries, 2006; Singer, 1999).

The latencies we observed for the face-selective N170 shared important electrophysiological properties with previous reports such as negative polarity and categorical selectivity to faces (Allison et al., 1994; Engell & McCarthy, 2011; McCarthy et al., 1999; Pourtois et al., 2010a). Models of hierarchical and differential encoding of face information have postulated that early perceptual effects in the N170 time range of 140–160 msec convey configurational analysis of faces, whereas effects between 180 and 200 msec reflect processing of facial identity (Eimer, 2000; Pourtois et al., 2010a). Changeable or behaviorally relevant aspects of faces, such as emotion and gaze, are processed between 310 and 1,000 msec according to these models. In line with this framework and previous reports (Allison et al., 1999; Halgren et al., 1994; McCarthy et al., 1999; Parvizi et al., 2012; Pourtois et al., 2010a; Puce et al., 1999; Tsuchiya et al., 2008), the earliest responses in the ERP around 100 msec were restricted to category-selective responses to faces or nonfaces, suggesting configurational analysis of the stimuli. In a similar vein, face-selective information in the human VOTC could be decoded as early as 100 msec, and this decoding was invariant to viewpoint or scale (Liu, Agam, Madsen, & Kreiman, 2009). In accordance with previous iEEG and ECoG studies, the response properties between adjacent recording sites in the VOTC were different (Kawasaki et al., 2012; Lachaux et al., 2005), suggesting narrowly circumscribed sources for preferential selectivity to faces and nonfaces.

All effects of facial expression, task-related attentional modulation, and their interaction were obtained considerably later than 160 msec in the present study, and were characterized by sustained GBA modulations. Consistent with our data, previous studies showed that effects of endogenous attention in the VOTC evolved only after 250 msec in both ERPs and GBA, whereas category-selective responses to faces and houses emerged earlier (Engell & McCarthy, 2010; Vidal et al., 2010). In line with our data, modulations by facial expressions have been observed previously in this region but only in a fraction of recording sites (Kawasaki et al., 2012). This result is also in agreement with results from temporal lobe face patches of nonhuman primates, in which effects of facial expression were only weak (Tsao, Schweers, et al., 2008). In conclusion, early responses in the VOTC around 100 msec were related to the stimulus category and insensitive to facial expression or task demands. Effects of facial expression or attentional modulation appeared after 200 msec.

4.2. VTC

Responses in the majority of sites in the VTC were modulated by endogenous attention. The gamma band response was different for faces and nonfaces exclusively during the explicit task between 500 and 700 msec. When faces were task-irrelevant, GBA responses were lower in amplitude and less sustained. Consistent with our results, similar latency and frequency ranges have been observed for detected *vs* undetected faces at recording sites in the inferior temporal gyrus (Lachaux et al., 2005). Our data suggest that face processing in the VTC is not automatic but that the VTC is primarily recruited whenever additional care must be given to faces.

Stronger GBA for faces in a subset of recording sites (4 out of 33) in the VTC, comparable to responses in the VOTC and irrespective of the task, is in agreement with the finding of face-selective regions towards the anterior pole in healthy populations (Weiner & Grill-Spector, 2013). Face patches in the anterior portion of the temporal lobe have been found in both human and nonhuman primates (Tsao, Moeller, et al., 2008). This result also confirms the role of the VTC in the core system of the face-processing network.

Consistent with our ERP results in the VTC, long-latency, face-specific potentials that were heterogeneous with respect to latency, waveform, and polarity were recorded previously (Allison et al., 1994, 1999; Puce et al., 1999). Such long-latency responses have partly been attributed to a phase reset of ongoing neuronal activity (Fell et al., 2004). Face-specific ERPs appear to be more heterogeneous and considerably later than responses in the GBA.

4.3. *Anterior insula*

GBA responses in the anterior insula initially increased to faces and nonfaces and were subsequently modulated by task demands beyond 200 msec, i.e., we found GBA increases for faces only in the explicit task. A similar effect was observed in the ERPs of another iEEG study, in which the potentials in the ventral anterior insula to the facial expression of disgust were more frequently observed and of longer duration during explicit than implicit emotion judgment (Krolak-Salmon et al., 2003). The unspecific onset responses suggest that the anterior insula, comparable to the core system, is initially active and subsequently upregulated by task demands. It has been proposed that the anterior insula detects salient stimuli and initiates appropriate control signals (Menon & Uddin, 2010).

A single site in the anterior insula exhibited initially increased GBA to fearful faces in both tasks. Although the anterior insula has been primarily implicated in the perception of disgust (Fusar-Poli et al., 2009; Phillips et al., 1998), increased neuronal activity to fearful faces has been observed previously in this region (Anderson, Christoff, Panitz, De Rosa, & Gabrieli, 2003; Morris et al., 1998). Similar to our results, Anderson et al. (2003) found a reduction of insular activity, when attention was directed away from faces. Altogether, these findings are consistent with a general role for the insula in coordinating sensorimotor responses to salient and unexpected stimuli (Augustine, 1996; Menon & Uddin, 2010).

4.4. *OFC*

Two different patterns of neuronal responses have been observed in distinct parts of the OFC that may be related to different cognitive processes. First, gamma band responses in lateral sites of the OFC were characterized by stronger gamma band suppression to faces compared to nonfaces in most sites, especially when faces were task-relevant. This effect is comparable to suppression of GBA in the OFC that has previously been observed during a visual search task (Ossandón et al., 2011) and during attentive reading (Lachaux et al., 2008). These findings have been interpreted as a task-related inhibition of background activity to maximize the level of performance. In both studies, the ventrolateral prefrontal cortex showed gamma band suppression when attention had to be oriented towards external stimuli. These findings accord well with the region, in which we observed suppressed GBA in the current study. Hence, the present result corroborates the role of task-specific GBA suppression for mediating goal-directed behavior.

Second, drawing on findings from object recognition, the remarkably early GBA increase in a medial site exclusively during explicit face processing in a single patient may reflect top-down facilitation of face perception (Adolphs, 2002). Bar et al. (2006) investigated the recognition of briefly presented, masked objects with fMRI and magnetoencephalography and observed that the OFC activation at 130 msec preceded that of the fusiform gyrus at 180–215 msec. Although the responses in the VOTC emerged earlier in our iEEG recordings, the latencies in the OFC are in good agreement with these data. Another study reported short-latency responses (120–160 msec) in single units in the right ventromedial prefrontal cortex that were selective for aversive visual stimuli (Kawasaki et al., 2001). This finding has been interpreted as reflecting rapid and coarse stimulus categorization. Greater prefrontal responses have also been found to attended but not unattended emotional prosody in functional neuroimaging in humans (Sander et al., 2005) and to expressive compared to neutral faces in electrophysiological recordings in monkeys (Tsao, Schweers, et al., 2008). Hence, our early increase of GBA in the OFC suggests that the OFC is involved in top-down facilitation of face perception (Adolphs, 2002) and the allocation of resources (Sakai, 2008).

4.5. *Amygdala*

The amygdala displayed stronger GBA for faces compared to nonfaces especially when processing of faces was task-relevant. This effect peaked between 350 and 450 msec after stimulus onset. The observed latencies are in line with the report of face-selective neurons in the monkey amygdala with a firing-rate increase between 100 and 300 msec (Gothard et al., 2007; Leonard et al., 1985). Importantly, latencies exceeding those in the VOTC and strong attenuation in the implicit task argue against an automatic activation of the amygdala when confronted with fearful faces (Palermo & Rhodes, 2007; Vuilleumier, 2002).

The amygdala is also consistently activated when neutral faces are contrasted to baseline (Fusar-Poli et al., 2009). To date, only few studies have investigated GBA in the amygdala with iEEG in humans. Increased GBA in the amygdala has been observed in response to unpleasant pictures, faces, fearful facial expressions, and solely the eyes of a face compared to different control stimuli (Oya, Kawasaki, Howard, & Adolphs, 2002; Sato et al., 2011a, 2011b, 2012). However, none of those studies examined whether the amygdala response could be modulated by task demands or endogenous attention. We propose that the increased GBA in the amygdala relates to higher salience of faces, when they are task-relevant. This interpretation is in line with proposals that the functional importance of the amygdala is not limited specifically to emotion but also comprises other abstract dimensions of information processing, such as salience (Adolphs, 2010; Pessoa & Adolphs, 2010). Furthermore, our finding of increased GBA to task-relevant faces in the amygdala accords well with the idea that the amygdala coordinates appropriate responses according to the relevance of a stimulus for the goals of the individual (Cunningham & Brosch, 2012; Sander et al., 2003).

Effects of fearful faces on the GBA and the ERPs in the amygdala were only found in one patient. This result conflicts with previous iEEG studies reporting higher ERP and GBA amplitudes for fearful compared to neutral faces (Krolak-Salmon et al., 2004; Pourtois et al., 2010b; Sato et al., 2011b)

and a large body of functional neuroimaging literature (Fusar-Poli et al., 2009; Morris et al., 1996; Zald, 2003). Pourtois et al. (2010b) found higher ERP amplitudes for fearful *vs* neutral faces 140 msec after stimulus onset irrespective of task-relevance in a single patient implanted in the lateral amygdala. Likewise, augmented potentials have been observed exclusively for fearful relative to other expressions (Krolak-Salmon et al., 2004), when attention had to be directed to facial expression. A possibility why emotion effects were only rarely observed in the present study is discussed in 4.6.

4.6. *Limitations*

In the explicit task, not only facial expression but likewise faces as stimulus category became task-relevant. This limitation of our experimental design may account for the small effects of facial expression. In order to draw attention to faces but not facial expression, previous research compared "attention to gender" with "attention to facial expression" (Krolak-Salmon et al., 2004; Monroe et al., 2013; Wronka & Walentowska, 2011). The present design does not allow disentangling effects specific to facial expression from those related to faces in general. Because it was sufficient to attend to the low-level feature red tint to identify targets in the implicit condition, facial features could be ignored so that the comparison of explicit and implicit conditions does not isolate attentional effects to facial expression. It rather informs about attentional effects to faces including facial expression. Hence, attentional effects to faces as stimulus category could have occluded those to facial expression, accounting for the small effects of facial expression in the present study. Still, the present study allows conclusions as to whether emotional faces capture attention automatically. If fearful faces had captured attention automatically, and such attentional capture had been specific to fearful relative to neutral faces, this would have resulted in differential neuronal responses (GBA, ABBA, ERP) between fearful and neutral faces, even when attention had not been intentionally directed to the expression, as in the implicit condition of the present study. Given that differences between fearful and neutral faces were marginal if not absent, we can conclude that fearful faces did not capture attention automatically.

Patients might have used a similar processing strategy in nontarget trials of the explicit and implicit tasks because they were requested to respond in only ten percent of the trials. Since targets were discarded from analysis, the two experimental blocks solely differed in the task instruction. No differences between these two would have been observed, if patients had used the same processing strategy in nontarget trials of both tasks. Therefore, the task-related neuronal effects support the assumption that patients indeed used explicit and implicit processing strategies in the respective tasks, and that our attentional manipulation was successful. As noted in the previous paragraph, the main effect of task reflects attentional effects generic to faces rather than effects specifically associated with facial expression.

Stimuli in explicit and implicit tasks differed in the presence of happy faces. Happy faces were only present as targets in the explicit task. Fearful faces might have been processed differently among happy and neutral faces compared to presentation among neutral faces only. Most likely, participants pay more attention to the facial expression of the face when both emotions are present as in the explicit condition of the present study. For this condition we hypothesized a stronger neuronal response because attention was explicitly directed to facial expression. Hence, if the presence of happy faces had impacted the present results at all, it would have been in the desired direction of our experimental manipulation.

4.7. *Conclusion*

In conclusion, our study demonstrated that all investigated regions of the face-processing network were clearly modulated by task demands and exhibited stronger changes in GBA when faces were task-relevant. The latencies we observed suggest an orchestrated activation in the face-processing network. The core system, including the VOTC and VTC, and the anterior insula, as part of the extended system, exhibited early responses around 100 msec, which were stimulus-specific to faces and nonfaces in the core system. Sustained GBA around 200 msec reflected effects of endogenous attention in the core system and the anterior insula, substantiating the role of the core system of face processing and indicating the allocation of attentional resources for further processing. In contrast, strong effects of endogenous attention in the OFC and amygdala beyond 300 msec support the notion that the extended system of the face-processing network is only recruited if the task requires active processing of facial expression. Our results show that endogenous attention operates in the whole face-processing network and that these effects are specifically reflected in frequency-specific changes in the gamma band.

Acknowledgments

We thank all the patients who participated in this study and the staff at the CHU Grenoble. Furthermore, we thank Tomás Ossandón and Juan R. Vidal for help in data analysis and Sarang S. Dalal for support in MRI coregistration. Grants from the German Research Foundation (SFB TRR58/B04, SFB936/A3, A.K.E.), the European Union (HEALTH-F2-2008-200728, A.K.E., J.P.L.; ERC-2010-AdG-269716, A.K.E), the G.A. Lienert Foundation (K.M.), the French National Research Agency (ANR-MLA ANR-10-BLAN-1409, J.P.L), and the French investissements d'avenir (LABEX CORTEX ANR-11-LABX-0042, J.P.L) supported this research. The funders had no role in study design, data collection and analysis, decision to publish, or preparation of the manuscript. The authors have declared that no competing interests exist.

REFERENCES

Adolphs, R. (2002). Recognizing emotion from facial expressions: psychological and neurological mechanisms. *Behavioral and Cognitive Neuroscience Reviews*, 1(1), 21–62.

Adolphs, R. (2010). What does the amygdala contribute to social cognition? *Annals of the New York Academy of Sciences, 1191*, 42–61.
Adolphs, R., Tranel, D., Damasio, H., & Damasio, A. (1994). Impaired recognition of emotion in facial expressions following bilateral damage to the human amygdala. *Nature, 372*(6507), 669–672.
Allison, T., McCarthy, G., Nobre, A., Puce, A., & Belger, A. (1994). Human extrastriate visual cortex and the perception of faces, words, numbers, and colors. *Cerebral Cortex, 4*(5), 544–554.
Allison, T., Puce, A., Spencer, D. D., & McCarthy, G. (1999). Electrophysiological studies of human face perception. I: potentials generated in occipitotemporal cortex by face and non-face stimuli. *Cerebral Cortex, 9*(5), 415–430.
Anderson, A. K., Christoff, K., Panitz, D., De Rosa, E., & Gabrieli, J. D. (2003). Neural correlates of the automatic processing of threat facial signals. *The Journal of Neuroscience, 23*(13), 5627–5633.
Augustine, J. R. (1996). Circuitry and functional aspects of the insular lobe in primates including humans. *Brain Research Reviews, 22*(3), 229–244.
Balconi, M., & Lucchiari, C. (2006). EEG correlates (event-related desynchronization) of emotional face elaboration: a temporal analysis. *Neuroscience Letters, 392*(1–2), 118–123.
Balconi, M., & Pozzoli, U. (2007). Event-related oscillations (EROs) and event-related potentials (ERPs) comparison in facial expression recognition. *Journal of Neuropsychology, 1*(Pt 2), 283–294.
Bar, M., Kassam, K. S., Ghuman, A. S., Boshyan, J., Schmid, A. M., Dale, A. M., et al. (2006). Top-down facilitation of visual recognition. *Proceedings of the National Academy of Sciences of the United States of America, 103*(2), 449–454.
Benjamini, Y., & Hochberg, Y. (1995). Controlling the false discovery rate – a practical and powerful approach to multiple testing. *Journal of the Royal Statistical Society – Series B: Methodological, 57*(1), 289–300.
Bentin, S., Allison, T., Puce, A., Perez, E., & McCarthy, G. (1996). Electrophysiological studies of face perception in humans. *Journal of Cognitive Neuroscience, 8*(6), 551–565.
Brosch, T., Grandjean, D., Sander, D., & Scherer, K. R. (2009). Cross-modal emotional attention: emotional voices modulate early stages of visual processing. *Journal of Cognitive Neuroscience, 21*(9), 1670–1679.
Canli, T., Sivers, H., Whitfield, S. L., Gotlib, I. H., & Gabrieli, J. D. (2002). Amygdala response to happy faces as a function of extraversion. *Science,, 296*(5576), 2191.
Cornwell, B. R., Carver, F. W., Coppola, R., Johnson, L., Alvarez, R., & Grillon, C. (2008). Evoked amygdala responses to negative faces revealed by adaptive MEG beamformers. *Brain Research, 1244*, 103–112.
Cunningham, W. A., & Brosch, T. (2012). Motivational salience: amygdala tuning from traits, needs, values, and goals. *Current Directions in Psychological Science, 21*(1).
Donner, T. H., & Siegel, M. (2011). A framework for local cortical oscillation patterns. *Trends in Cognitive Sciences, 15*(5), 191–199.
Eimer, M. (2000). Event-related brain potentials distinguish processing stages involved in face perception and recognition. *Clinical Neurophysiology, 111*(4), 694–705.
Engel, A. K., Fries, P., & Singer, W. (2001). Dynamic predictions: oscillations and synchrony in top–down processing. *Nature Reviews Neuroscience, 2*(10), 704–716.
Engell, A. D., & McCarthy, G. (2010). Selective attention modulates face-specific induced gamma oscillations recorded from ventral occipitotemporal cortex. *The Journal of Neuroscience, 30*(26), 8780–8786.
Engell, A. D., & McCarthy, G. (2011). The relationship of gamma oscillations and face-specific ERPs recorded subdurally from occipitotemporal cortex. *Cerebral Cortex, 21*(5), 1213–1221.
Evans, A. C., Collins, D. L., Mills, S. R., Brown, E. D., Kelly, R. L., & Peters, T. M. (1993). 3D statistical neuroanatomical models from 305 MRI volumes. In *Nuclear Science Symposium and Medical Imaging Conference, IEEE Conference Record* (pp. 1813–1817).
Fell, J., Dietl, T., Grunwald, T., Kurthen, M., Klaver, P., Trautner, P., et al. (2004). Neural bases of cognitive ERPs: more than phase reset. *Journal of Cognitive Neuroscience, 16*(9), 1595–1604.
Fenker, D. B., Heipertz, D., Boehler, C. N., Schoenfeld, M. A., Noesselt, T., Heinze, H. J., et al. (2010). Mandatory processing of irrelevant fearful face features in visual search. *Journal of Cognitive Neuroscience, 22*(12), 2926–2938.
Fries, P., Reynolds, J. H., Rorie, A. E., & Desimone, R. (2001). Modulation of oscillatory neuronal synchronization by selective visual attention. *Science, 291*(5508), 1560–1563.
Fusar-Poli, P., Placentino, A., Carletti, F., Landi, P., Allen, P., Surguladze, S., et al. (2009). Functional atlas of emotional faces processing: a voxel-based meta-analysis of 105 functional magnetic resonance imaging studies. *Journal of Psychiatry and Neuroscience, 34*(6), 418–432.
Gao, Z., Goldstein, A., Harpaz, Y., Hansel, M., Zion-Golumbic, E., & Bentin, S. (2013). A magnetoencephalographic study of face processing: M170, gamma-band oscillations and source localization. *Human Brain Mapping, 34*(8), 1783–1795.
Gobbini, M. I., & Haxby, J. V. (2007). Neural systems for recognition of familiar faces. *Neuropsychologia, 45*(1), 32–41.
Gothard, K. M., Battaglia, F. P., Erickson, C. A., Spitler, K. M., & Amaral, D. G. (2007). Neural responses to facial expression and face identity in the monkey amygdala. *Journal of Neurophysiology, 97*(2), 1671–1683.
Grandjean, D., Sander, D., Lucas, N., Scherer, K. R., & Vuilleumier, P. (2008). Effects of emotional prosody on auditory extinction for voices in patients with spatial neglect. *Neuropsychologia, 46*(2), 487–496.
Halgren, E., Baudena, P., Heit, G., Clarke, J. M., Marinkovic, K., & Clarke, M. (1994). Spatio-temporal stages in face and word processing. I. Depth-recorded potentials in the human occipital, temporal and parietal lobes [corrected]. *Journal of Physiology, 88*(1), 1–50.
Haxby, J. V., Hoffman, E. A., & Gobbini, M. I. (2000). The distributed human neural system for face perception. *Trends in Cognitive Sciences, 4*(6), 223–233.
Hipp, J. F., Engel, A. K., & Siegel, M. (2011). Oscillatory synchronization in large-scale cortical networks predicts perception. *Neuron, 69*(2), 387–396.
Hoffman, K. L., Gothard, K. M., Schmid, M. C., & Logothetis, N. K. (2007). Facial-expression and gaze-selective responses in the monkey amygdala. *Current Biology, 17*(9), 766–772.
Hoogenboom, N., Schoffelen, J. M., Oostenveld, R., Parkes, L. M., & Fries, P. (2006). Localizing human visual gamma-band activity in frequency, time and space. *NeuroImage, 29*(3), 764–773.
Ishai, A., Schmidt, C. F., & Boesiger, P. (2005). Face perception is mediated by a distributed cortical network. *Brain Research Bulletin, 67*(1–2), 87–93.
Jensen, O., Kaiser, J., & Lachaux, J. P. (2007). Human gamma-frequency oscillations associated with attention and memory. *Trends in Neurosciences, 30*(7), 317–324.
Jerbi, K., Freyermuth, S., Dalal, S., Kahane, P., Bertrand, O., Berthoz, A., et al. (2009). Saccade related gamma-band activity in intracerebral EEG: dissociating neural from ocular muscle activity. *Brain Topography, 22*(1), 18–23.
Jerbi, K., Ossandón, T., Hamamé, C. M., Senova, S., Dalal, S. S., Jung, J., et al. (2009). Task-related gamma-band dynamics from an intracerebral perspective: review and implications for surface EEG and MEG. *Human Brain Mapping, 30*(6), 1758–1771.
Kanwisher, N., McDermott, J., & Chun, M. M. (1997). The fusiform face area: a module in human extrastriate cortex specialized for face perception. *The Journal of Neuroscience, 17*(11), 4302–4311.

Kawasaki, H., Kaufman, O., Damasio, H., Damasio, A. R., Granner, M., Bakken, H., et al. (2001). Single-neuron responses to emotional visual stimuli recorded in human ventral prefrontal cortex. *Nature Neuroscience, 4*(1), 15–16.

Kawasaki, H., Tsuchiya, N., Kovach, C. K., Nourski, K. V., Oya, H., Howard, M. A., et al. (2012). Processing of facial emotion in the human fusiform gyrus. *Journal of Cognitive Neuroscience, 24*(6), 1358–1370.

Kreifelts, B., Ethofer, T., Grodd, W., Erb, M., & Wildgruber, D. (2007). Audiovisual integration of emotional signals in voice and face: an event-related fMRI study. *NeuroImage, 37*(4), 1445–1456.

Krolak-Salmon, P., Hénaff, M. A., Isnard, J., Tallon-Baudry, C., Guenot, M., Vighetto, A., et al. (2003). An attention modulated response to disgust in human ventral anterior insula. *Annals of Neurology, 53*(4), 446–453.

Krolak-Salmon, P., Hénaff, M. A., Vighetto, A., Bertrand, O., & Mauguière, F. (2004). Early amygdala reaction to fear spreading in occipital, temporal, and frontal cortex: a depth electrode ERP study in human. *Neuron, 42*(4), 665–676.

Lachaux, J. P., Axmacher, N., Mormann, F., Halgren, E., & Crone, N. E. (2012). High-frequency neural activity and human cognition: past, present and possible future of intracranial EEG research. *Progress in Neurobiology, 98*(3), 279–301.

Lachaux, J. P., Fonlupt, P., Kahane, P., Minotti, L., Hoffmann, D., Bertrand, O., et al. (2007). Relationship between task-related gamma oscillations and BOLD signal: new insights from combined fMRI and intracranial EEG. *Human Brain Mapping, 28*(12), 1368–1375.

Lachaux, J. P., George, N., Tallon-Baudry, C., Martinerie, J., Hugueville, L., Minotti, L., et al. (2005). The many faces of the gamma band response to complex visual stimuli. *NeuroImage, 25*(2), 491–501.

Lachaux, J. P., Jung, J., Mainy, N., Dreher, J. C., Bertrand, O., Baciu, M., et al. (2008). Silence is golden: transient neural deactivation in the prefrontal cortex during attentive reading. *Cerebral Cortex, 18*(2), 443–450.

Lachaux, J. P., Rudrauf, D., & Kahane, P. (2003). Intracranial EEG and human brain mapping. *Journal of Physiology, 97*(4–6), 613–628.

Le Van Quyen, M., Foucher, J., Lachaux, J., Rodriguez, E., Lutz, A., Martinerie, J., et al. (2001). Comparison of Hilbert transform and wavelet methods for the analysis of neuronal synchrony. *The Journal of Neuroscience Methods, 111*(2), 83–98.

Leonard, C. M., Rolls, E. T., Wilson, F. A., & Baylis, G. C. (1985). Neurons in the amygdala of the monkey with responses selective for faces. *Behavioural Brain Research, 15*(2), 159–176.

Liu, H., Agam, Y., Madsen, J. R., & Kreiman, G. (2009). Timing, timing, timing: fast decoding of object information from intracranial field potentials in human visual cortex. *Neuron, 62*(2), 281–290.

Logothetis, N. K., Pauls, J., Augath, M., Trinath, T., & Oeltermann, A. (2001). Neurophysiological investigation of the basis of the fMRI signal. *Nature, 412*(6843), 150–157.

Lundqvist, D., Flykt, A., & Öhman, A. (1998). *The Karolinska directed emotional faces – KDEF. CD ROM from Department of Clinical Neuroscience, Psychology Section, Karolinska Institute*.

Macmillan, N. A., & Creelman, C. D. (1991). *Detection theory: a user's guide*. Cambridge [England] ; New York: Cambridge University Press.

Manning, J. R., Jacobs, J., Fried, I., & Kahana, M. J. (2009). Broadband shifts in local field potential power spectra are correlated with single-neuron spiking in humans. *The Journal of Neuroscience, 29*(43), 13613–13620.

McCarthy, G., Puce, A., Belger, A., & Allison, T. (1999). Electrophysiological studies of human face perception. II: response properties of face-specific potentials generated in occipitotemporal cortex. *Cerebral Cortex, 9*(5), 431–444.

Menon, V., & Uddin, L. Q. (2010). Saliency, switching, attention and control: a network model of insula function. *Brain Structure and Function, 214*(5–6), 655–667.

Mitra, P. P., & Pesaran, B. (1999). Analysis of dynamic brain imaging data. *Biophysical Journal, 76*(2), 691–708.

Monroe, J. F., Griffin, M., Pinkham, A., Loughead, J., Gur, R. C., Roberts, T. P., et al. (2013). The fusiform response to faces: explicit versus implicit processing of emotion. *Human Brain Mapping, 34*(1), 1–11.

Morris, J. S., Friston, K. J., Büchel, C., Frith, C. D., Young, A. W., Calder, A. J., et al. (1998). A neuromodulatory role for the human amygdala in processing emotional facial expressions. *Brain, 121*(Pt 1), 47–57.

Morris, J. S., Frith, C. D., Perrett, D. I., Rowland, D., Young, A. W., Calder, A. J., et al. (1996). A differential neural response in the human amygdala to fearful and happy facial expressions. *Nature, 383*(6603), 812–815.

Öhman, A., & Mineka, S. (2001). Fears, phobias, and preparedness: toward an evolved module of fear and fear learning. *Psychological Review, 108*(3), 483–522.

Oostenveld, R., Fries, P., Maris, E., & Schoffelen, J. M. (2011). FieldTrip: open source software for advanced analysis of MEG, EEG, and invasive electrophysiological data. *Computational Intelligence and Neuroscience, 2011*, 156869.

Ossandón, T., Jerbi, K., Vidal, J. R., Bayle, D. J., Hénaff, M. A., Jung, J., et al. (2011). Transient suppression of broadband gamma power in the default-mode network is correlated with task complexity and subject performance. *The Journal of Neuroscience, 31*(41), 14521–14530.

Ossandón, T., Vidal, J. R., Ciumas, C., Jerbi, K., Hamamé, C. M., Dalal, S. S., et al. (2012). Efficient "pop-out" visual search elicits sustained broadband gamma activity in the dorsal attention network. *The Journal of Neuroscience, 32*(10), 3414–3421.

Oya, H., Kawasaki, H., Howard, M. A., & Adolphs, R. (2002). Electrophysiological responses in the human amygdala discriminate emotion categories of complex visual stimuli. *The Journal of Neuroscience, 22*(21), 9502–9512.

Palermo, R., & Rhodes, G. (2007). Are you always on my mind? A review of how face perception and attention interact. *Neuropsychologia, 45*(1), 75–92.

Parvizi, J., Jacques, C., Foster, B. L., Witthoft, N., Rangarajan, V., Weiner, K. S., et al. (2012). Electrical stimulation of human fusiform face-selective regions distorts face perception. *The Journal of Neuroscience, 32*(43), 14915–14920.

Pessoa, L., & Adolphs, R. (2010). Emotion processing and the amygdala: from a 'low road' to 'many roads' of evaluating biological significance. *Nature Reviews Neuroscience, 11*(11), 773–783.

Phan, K. L., Wager, T., Taylor, S. F., & Liberzon, I. (2002). Functional neuroanatomy of emotion: a meta-analysis of emotion activation studies in PET and fMRI. *NeuroImage, 16*(2), 331–348.

Phillips, M. L., Young, A. W., Scott, S. K., Calder, A. J., Andrew, C., Giampietro, V., et al. (1998). Neural responses to facial and vocal expressions of fear and disgust. *Proceedings of the Royal Society B: Biological Sciences, 265*(1408), 1809–1817.

Pourtois, G., Spinelli, L., Seeck, M., & Vuilleumier, P. (2010a). Modulation of face processing by emotional expression and gaze direction during intracranial recordings in right fusiform cortex. *Journal of Cognitive Neuroscience, 22*(9), 2086–2107.

Pourtois, G., Spinelli, L., Seeck, M., & Vuilleumier, P. (2010b). Temporal precedence of emotion over attention modulations in the lateral amygdala: Intracranial ERP evidence from a patient with temporal lobe epilepsy. *Cognitive Affective & Behavioral Neuroscience, 10*(1), 83–93.

Puce, A., Allison, T., & McCarthy, G. (1999). Electrophysiological studies of human face perception. III: Effects of top–down Processing on Face-specific Potentials. *Cerebral Cortex, 9*(5), 445–458.

Ray, S., & Maunsell, J. H. (2011). Different origins of gamma rhythm and high-gamma activity in macaque visual cortex. *PLoS Biology, 9*(4), e1000610.
Rodriguez, E., George, N., Lachaux, J. P., Martinerie, J., Renault, B., & Varela, F. J. (1999). Perception's shadow: long-distance synchronization of human brain activity. *Nature, 397*(6718), 430–433.
Rolls, E. T. (2004). The functions of the orbitofrontal cortex. *Brain and Cognition, 55*(1), 11–29.
Russell, J. A. (1994). Is there universal recognition of emotion from facial expression? A review of the cross-cultural studies. *Psychological Bulletin, 115*(1), 102–141.
Rutishauser, U., Tudusciuc, O., Neumann, D., Mamelak, A. N., Heller, A. C., Ross, I. B., et al. (2011). Single-unit responses selective for whole faces in the human amygdala. *Current Biology,, 21*(19), 1654–1660.
Sakai, K. (2008). Task set and prefrontal cortex. *Annual Review of Neuroscience, 31*, 219–245.
Sander, D., Grafman, J., & Zalla, T. (2003). The human amygdala: an evolved system for relevance detection. *Reviews in the Neurosciences, 14*(4), 303–316.
Sander, D., Grandjean, D., Pourtois, G., Schwartz, S., Seghier, M. L., Scherer, K. R., et al. (2005). Emotion and attention interactions in social cognition: brain regions involved in processing anger prosody. *NeuroImage, 28*(4), 848–858.
Sato, W., Kochiyama, T., Uono, S., Matsuda, K., Usui, K., Inoue, Y., et al. (2011a). Rapid amygdala gamma oscillations in response to eye gaze. *PLoS One, 6*(11), e28188.
Sato, W., Kochiyama, T., Uono, S., Matsuda, K., Usui, K., Inoue, Y., et al. (2011b). Rapid amygdala gamma oscillations in response to fearful facial expressions. *Neuropsychologia, 49*(4), 612–617.
Sato, W., Kochiyama, T., Uono, S., Matsuda, K., Usui, K., Inoue, Y., et al. (2012). Temporal profile of amygdala gamma oscillations in response to faces. *Journal of Cognitive Neuroscience, 24*(6), 1420–1433.
Siegel, M., Donner, T. H., & Engel, A. K. (2012). Spectral fingerprints of large-scale neuronal interactions. *Nature Reviews Neuroscience, 13*(2), 121–134.
Siegel, M., Donner, T. H., Oostenveld, R., Fries, P., & Engel, A. K. (2008). Neuronal Synchronization along the dorsal visual pathway reflects the focus of spatial attention. *Neuron, 60*(4), 709–719.
Singer, W. (1999). Neuronal synchrony: a versatile code for the definition of relations? *Neuron, 24*(1), 49–65, 111–125.
Tallon-Baudry, C., & Bertrand, O. (1999). Oscillatory gamma activity in humans and its role in object representation. *Trends in Cognitive Sciences, 3*(4), 151–162.
Tsao, D. Y., Freiwald, W. A., Tootell, R. B., & Livingstone, M. S. (2006). A cortical region consisting entirely of face-selective cells. *Science, 311*(5761), 670–674.
Tsao, D. Y., & Livingstone, M. S. (2008). Mechanisms of face perception. *Annual Review of Neuroscience, 31*, 411–437.
Tsao, D. Y., Moeller, S., & Freiwald, W. A. (2008). Comparing face patch systems in macaques and humans. *Proceedings of the National Academy of Sciences of the United States of America, 105*(49), 19514–19519.
Tsao, D. Y., Schweers, N., Moeller, S., & Freiwald, W. A. (2008). Patches of face-selective cortex in the macaque frontal lobe. *Nature Neuroscience, 11*(8), 877–879.
Tsuchiya, N., Kawasaki, H., Oya, H., Howard, M. A., 3rd, & Adolphs, R. (2008). Decoding face information in time, frequency and space from direct intracranial recordings of the human brain. *PLoS One, 3*(12), e3892.
Tzourio-Mazoyer, N., Landeau, B., Papathanassiou, D., Crivello, F., Etard, O., Delcroix, N., et al. (2002). Automated anatomical labeling of activations in SPM using a macroscopic anatomical parcellation of the MNI MRI single-subject brain. *NeuroImage, 15*(1), 273–289.
Vidal, J. R., Ossandón, T., Jerbi, K., Dalal, S. S., Minotti, L., Ryvlin, P., et al. (2010). Category-specific visual responses: an intracranial study comparing gamma, beta, alpha, and ERP response selectivity. *Frontiers in Human Neuroscience, 4*, 195.
Vuilleumier, P. (2002). Facial expression and selective attention. *Current Opinion in Psychiatry, 15*(3), 291–300.
Vuilleumier, P. (2005). How brains beware: neural mechanisms of emotional attention. *Trends in Cognitive Sciences, 9*(12), 585–594.
Vuilleumier, P., & Pourtois, G. (2007). Distributed and interactive brain mechanisms during emotion face perception: evidence from functional neuroimaging. *Neuropsychologia, 45*(1), 174–194.
Vuilleumier, P., Richardson, M. P., Armony, J. L., Driver, J., & Dolan, R. J. (2004). Distant influences of amygdala lesion on visual cortical activation during emotional face processing. *Nature Neuroscience, 7*(11), 1271–1278.
Weiner, K. S., & Grill-Spector, K. (2013). Neural representations of faces and limbs neighbor in human high-level visual cortex: evidence for a new organization principle. *Psychological Research, 77*(1), 74–97.
Wickens, T. D. (2002). *Elementary signal detection theory*. Oxford; New York: Oxford University Press.
Wronka, E., & Walentowska, W. (2011). Attention modulates emotional expression processing. *Psychophysiology, 48*(8), 1047–1056.
Zald, D. H. (2003). The human amygdala and the emotional evaluation of sensory stimuli. *Brain Research Reviews, 41*(1), 88–123.
Zion-Golumbic, E., & Bentin, S. (2007). Dissociated neural mechanisms for face detection and configural encoding: evidence from N170 and induced gamma-band oscillation effects. *Cerebral Cortex, 17*(8), 1741–1749.